

The structure and function of the nematocysts of *Chironex fleckeri* Southcott, 1956

J. Rifkin and R. Endean

Department of Zoology, University of Queensland, Brisbane, Queensland, Australia

Summary. Microbasic p-mastigophores, euryteles of two size groups, holotrichous isorhizas and atrichous isorhizas, comprise the cnidom of *Chironex fleckeri*, a cubozoan that has been responsible for several human fatalities. In its undischarged state each microbasic mastigophore of *C. fleckeri* consists of a capsule containing matrix and an inverted tube possessing a smooth-walled butt which is loosely coiled helically and which narrows to form a thread that is tightly coiled helically and markedly pleated. Both butt and thread carry three helices of spines and contain a granular matrix. During discharge, the proximal butt spines form initially a piercing stylet. Granular material from the butt and thread is released prior to the release of capsular material. Each eurytele possesses a tube with a butt composed of three bulbs, the middle bulb bearing long spines. Each holotrichous isorhiza possesses a coiled tube bearing small spines along its length. Each atrichous isorhiza exhibits a tube that is devoid of spines and loosely folded in the undischarged condition. The probable role of each type of nematocyst is inferred from its structure and features that enable the ready separation of the nematocysts of *C. fleckeri* from those of scyphozoan jellyfish are discussed.

Key words: Nematocysts – Structure – Ultrastructure – Function – Cubozoa

Send offprint requests to: J. Rifkin, Department of Zoology, University of Queensland, Brisbane, Queensland, Australia

Acknowledgement. We gratefully acknowledge the technical assistance given by Mr. J. Hardy of the Electron Microscope Unit, University of Queensland and by Mrs. L. Daddow and Mr. W. Stablum. We are indebted to Mr. A. Hansen of Proserpine for assistance with the collection of *Chironex fleckeri* and to Mrs. L.A. Pryor for assistance with drawings of nematocysts.

Chironex fleckeri is a jellyfish which possesses large nematocysts whose threads are capable of penetrating human skin. It has been responsible for numerous fatalities and near-fatalities in tropical Australian waters (Cleland and Southcott 1965; Barnes 1966; Williamson et al. 1980; Edean 1981). At least four basic types of nematocyst comprise the cnidom of *C. fleckeri* (Edean et al. 1969). The precise modes of operation and the respective roles of these different types are not known. However, an understanding of these aspects has implications for the first-aid treatment of human envenomations and for the preparation of extracts of nematocyst toxin to be used in pharmacological studies. To obtain this understanding it will first be necessary to examine details of the structure of each type of nematocyst. This paper reports on studies made on the structure, including ultrastructure, of discharged and undischarged nematocysts which throw some light on the mode of operation and the role of each nematocyst type.

Materials and methods

Mature specimens of *Chironex fleckeri* were collected at Repulse Bay in Central Queensland. Portions of their tentacles, about 1 cm in length, were stretched, fixed in 10% formalin, washed with distilled water, dehydrated in ethyl alcohol of increasing strength and then placed in a series of iso-amyl acetate solutions of increasing strength. Next they were dried in a critical-point drier (Denton). After drying they were coated with aluminium and examined with a Cambridge Stereoscan 600 or a Cambridge Stereoscan 2A electron microscope.

Suspensions consisting of mixed types of nematocyst from *C. fleckeri* isolated according to the method of Edean et al. (1969) were used for some observations with the phase-contrast microscope, the scanning electron microscope (SEM) and with the Siemens Elmiscope IA transmission electron microscope (TEM). For other observations the mixed nematocysts were separated into discrete types by density gradient centrifugation prior to examination (Edean and Rifkin 1975). In some cases drops of nematocyst suspension were placed on slides and either examined directly with the phase contrast microscope or exposed to 10% formalin, washed and stained with Mallory's trichrome stain before examination with the optical microscope. Other drops of nematocyst suspension were dehydrated in an ascending series of ethyl alcohol, placed in iso-amyl acetate and then in a critical point dryer. Next they were coated with aluminium and examined with the SEM.

In preparation for examination with the TEM suspensions of isolated nematocysts, both mixed and separated into different types as described above, were fixed in 4% glutaraldehyde in 0.1 M sucrose cacodylate buffer (pH = 7.2) for 2.5 h and then transferred to sucrose cacodylate buffer for 24 h. Then they were postfixing in 1% osmium tetroxide in 0.1 M sucrose cacodylate for 2 h before being thoroughly washed in 25% ethyl alcohol. Dehydration was accomplished by exposing the nematocyst pellet to each of a series of ethyl alcohols of increasing strength (10 min in each case). The pellet was next immersed in 100% ethyl alcohol for 30 min followed by embedding in Spurr's epoxy resin (Spurr 1969). Alternatively the pellet was transferred to propylene oxide for 30 min (2 changes) before being placed in a mixture of propylene oxide and Araldite resin for 16 h and finally embedded in Araldite resin. Silver-gray sections were cut using an LKB Ultratome III. In other cases suspensions of isolated nematocysts and short lengths (1 cm) of living tentacle were fixed in 3% glutaraldehyde in 0.1 M phosphate buffer at 4° C and at pH 7.3. After rinsing in phosphate buffer the nematocyst suspensions and tentacle portions were postfixing in 1% osmium tetroxide in 0.1 M phosphate buffer, washed in 0.1 M phosphate buffer, dehydrated with alcohol of increasing strength and then embedded in Spurr's epoxy resin. Silver-grey sections were cut on an Ultratome IV, stained with a saturated (10%) solution of uranyl acetate (40 min) and Reynold's lead citrate (20 min) and examined with a Siemens Elmiscope IA and an Hitachi H300 electron microscope.

Results

Microbasic p-mastigophores

These nematocysts possess a characteristic shape (Figs. 1, 24). Those measured range from 22.0 to 90 μm (mean = 54 μm) in length and from 7.0 to 10 μm (mean = 8.5 μm) at their greatest diameter (100 measurements in each case). Essentially, each nematocyst consists of a capsule containing a fine tube which bears spines. The tube arises from the broader end of the capsule and extends almost the full length of the capsule as a stiffened butt which is about 2 μm in diameter and which is coiled loosely to form a helix (Figs. 4, 24a). The butt merges with the remainder of the tube which constitutes the thread. The thread is about 1 μm in diameter and, when inverted inside the capsule, is tightly coiled helically (Fig. 4 inset). It makes two or three circuits of the capsule. The end of the thread distal to the butt appears, in some cases at least, to be attached to the wall of the capsule at its narrow end (Fig. 24a). A V-shaped notch can be seen in the undischarged tube at the point where the thread merges with the butt. The presence of this notch enables the mastigophores to be designated microbasic p-mastigophores (Carlgren 1940).

Under the SEM the walls of the capsule appear smooth and devoid of features except for one area at the broad end of the mastigophore through which the tube is eventually discharged. This area is surmounted by the opercular flap which is shaped like a clover-leaf (Fig. 2). Upon discharge of the mastigophore the flap is forced to one side (Figs. 3, 24b) as the basal portion of the butt emerges. During discharge, the tube everts beginning at the basal end and the butt with its spines appears (Fig. 24b). The first spines to appear form a piercing structure temporarily (Fig. 3). The butt spines are in three rows (Fig. 5), each row being separated by a groove from the neighbouring row and the rows themselves are helically arranged along the length of the butt (Fig. 5). The spines range up to 6 μm in length and each approximates the form of an isosceles triangle (Fig. 7). A scar is left at the point of attachment of a spine when it is detached. The thread, which is markedly pleated and tightly coiled, carries three rows of fine spines which are helically arranged and separated by grooves (Figs. 6, 8). Each thread spine approximates an equilateral triangle with a side of up to 0.6 μm .

In sections viewed with the TEM only one layer is apparent in the capsule walls of isolated nematocysts. However, the walls of nematocysts *in situ* are multilayered (Figs. 14, 23). The capsule walls of isolated mastigophores are up to 0.7 μm in thickness. The opening in the capsule at the base of the inverted tube found within each capsule is occluded by the tri-lobed opercular flap (Fig. 24a) comprised of electron-dense material (Fig. 9) with a marked periodicity resembling that of collagen. The flange in which the flap is seated appears to be composed of material different from the flap and different from the rest of the capsule wall. The wall

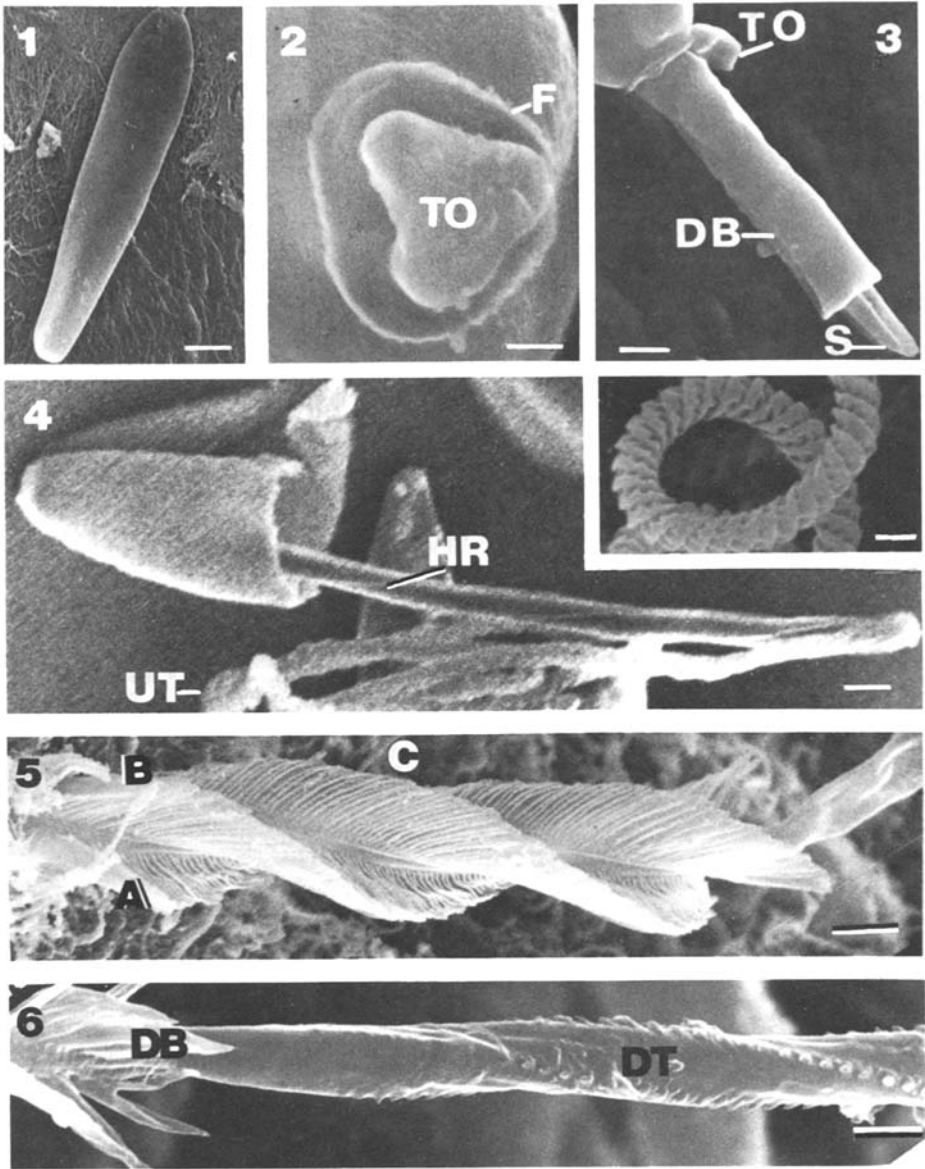


Fig. 1. Scanning electron micrograph of a microbasid mastigophore capsule. $\times 1077$. Bar = 8 μm

Fig. 2. Tripartite operculum (*TO*) and surrounding flange (*F*) of a microbasid mastigophore. $\times 13440$. Bar = 0.5 μm

Fig. 3. Partially discharged microbasid mastigophore showing tripped tripartite operculum (*TO*), discharged butt region (*DB*) devoid of spines, and emerging spines (*S*). $\times 3686$. Bar = 1.7 μm

Fig. 4. Ruptured microbasid mastigophore capsule showing helical ridges (*HR*) on undischarged butt, and undischarged thread (*UT*). $\times 1983$. Bar = 6 μm . *Inset*: arrangement of undischarged thread. $\times 9072$. Bar = 0.5 μm

Fig. 5. Discharged microbasid mastigophore butt showing three helices of spines. $\times 2800$. Bar = 2.9 μm

Fig. 6. Transition area between butt (*DB*) and thread (*DT*). $\times 3700$. Bar = 2.4 μm

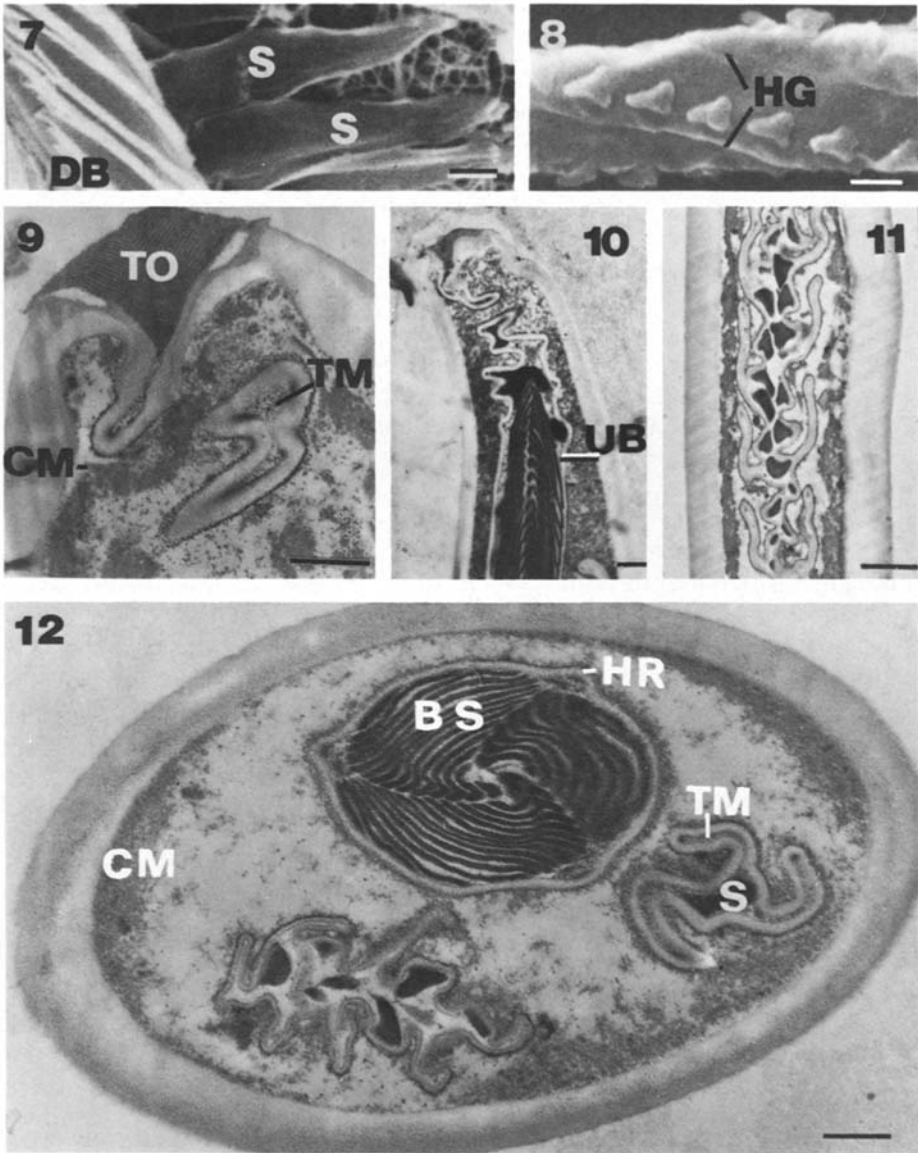


Fig. 8. Small spines of a microbasal mastigophore thread, arranged along helical grooves (*HG*). $\times 10000$. Bar = $0.7 \mu\text{m}$

Fig. 9. Longitudinal section through apical region of microbasal mastigophore showing periodicity in tripartite operculum (*TO*), spineless region of butt, granular tube matrix (*TM*) and capsular matrix (*CM*). $\times 15000$. Bar = $0.73 \mu\text{m}$

Fig. 10. Longitudinal section through microbasal mastigophore emphasizing the lack of pleating and folding of the undischarged butt wall (*UB*), and spines within. $\times 2000$. Bar = $2.0 \mu\text{m}$

Fig. 11. Longitudinal section through thread of microbasal mastigophore showing arrangement of thread spines within the deeply pleated and folded thread wall. $\times 5089$. Bar = $1.5 \mu\text{m}$

Fig. 12. Transverse section through microbasal mastigophore showing butt containing three helices of spines (*BS*) within; the helical ridges (*HR*) on the butt, and the spines (*S*) within the thread. Note also the tube matrix (*TM*) within the thread and the capsular matrix (*CM*). $\times 17714$. Bar = $0.5 \mu\text{m}$

of the tube appears to be continuous with the material of the flange (Fig. 9). That region of the butt nearest the operculum is devoid of spines. These appear at a point about a tenth the distance along the length of the butt from the opercular flap and their free ends point towards the operculum (Fig. 24b). Their general arrangement on the butt is illustrated in Figs. 10, 24b. Between the butt and the thread is a short region (Fig. 6) that is devoid of spines. Three ridges run helically along the length of the undischarged tube (Figs. 4, 12). In transverse section the thread is propeller-shaped (Fig. 12) because of the presence of pleats and folds. The thread spines appear as electron-dense structures; their arrangements can be clearly seen in Fig. 8. The capsule contents are comprised of granular as well as amorphous material. Electron-dense granular material is present in the lumen of the tube (Fig. 12).

During discharge the operculum at the broad end of the nematocyst opens and the tube everts through the hole formerly covered by the operculum (Fig. 24b). The tube rotates as it everts. This rotation probably stems from the manner in which the undischarged tube is coiled (Picken and Skaer 1966). The butt appears first and the butt spines emerge as the tube everts (Fig. 3). The butt is usually about the same length as the capsule. Subsequently the thread which bears minute spines appears (Figs. 6, 8). When fully everted (Fig. 24d) the thread ranges from 125 to 546 μm in length and is usually about six times the length of the capsule. With Mallory's triple dye, the capsular matrix was usually dyed light blue, and tube contents were dyed a red colour. Variations in the pattern of staining observed were probably related to the state of maturity of the nematocyst.

Heterotrichous microbasica euryteles

These occur in two size groups, one possessing long axes ranging from 29.5 to 39.0 μm (mean = 34 μm) and short axes ranging from 13.0 to 24.0 μm (mean = 17.0 μm) while the long axes of the other range from 8.0 to 16.5 μm (mean 12.0 μm) with short axes from 8.0 to 10.0 μm with a mean of 9.0 μm (100 measurements in each case). Each eurytele consists of a capsule containing an inverted tube which carries spines and which is differentiated into a butt and thread. However, the butt dilates when everted and forms three bulb-like structures, the second of which carries prominent spines (Figs. 13, 25d). This is reflected in the prominent folding exhibited by this region of the undischarged butt. Typically there are three deep pleats which are helically arranged on the butt (Figs. 14, 25a, b, c). The thread has a smaller diameter than the butt. Like the butt, it possesses extensive pleating (Figs. 14, 25b). The thread usually makes several circuits inside the capsule, and has been found attached to the capsule. The thread matrix was relatively homogeneous and the capsular matrix also appeared to be relatively homogeneous.

SEM reveals that the outer walls of the isolated capsules of the larger category of euryteles are ellipsoidal and smooth except for the presence of a distinct flange that surrounds the tripartite operculum. The walls of isolated capsules of the smaller category of euryteles are also smooth, but

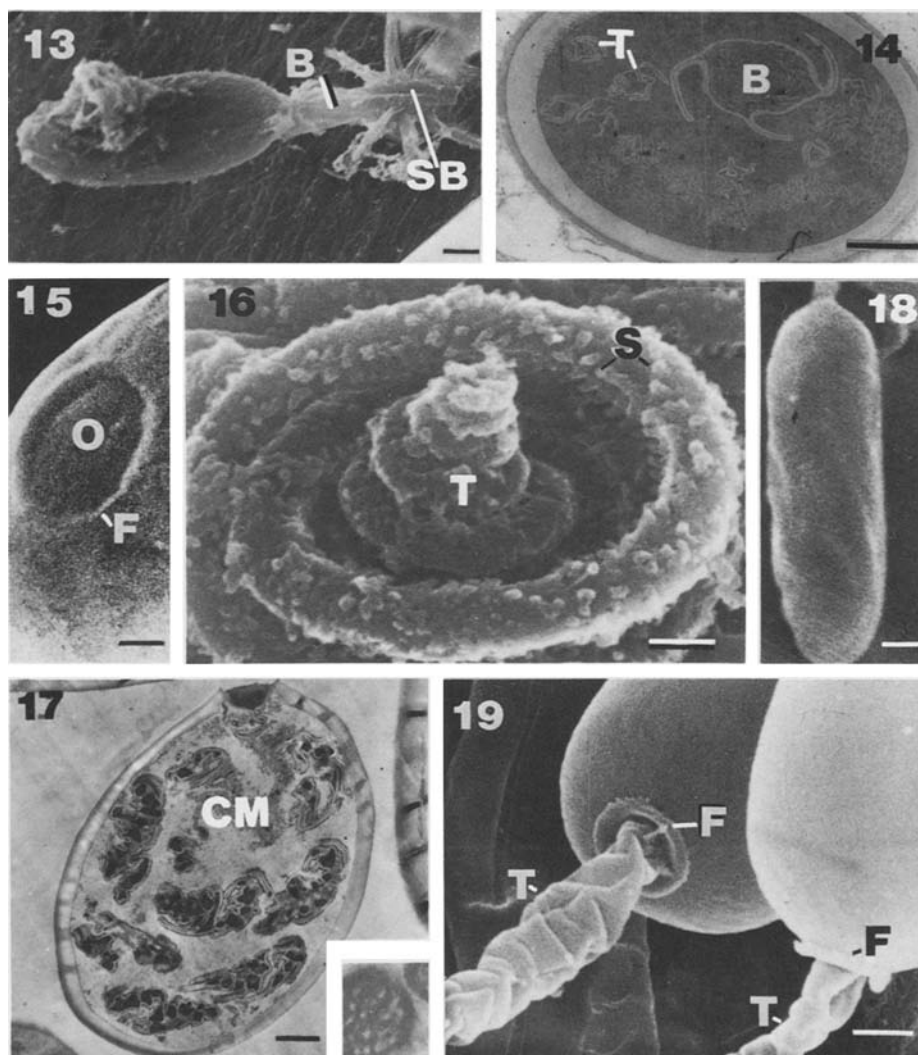


Fig. 13. Scanning electron micrograph showing a large heterotranchous microbasic eurytele penetrating human skin. Note first spineless bulb (*B*), and second, spiny bulb (*SB*). Third bulb and thread are buried in skin. $\times 1250$. Bar = $3.2 \mu\text{m}$

Fig. 14. Transverse section through eurytele in situ in tentacle showing deep pleats of spiny region of butt (*B*), and deeply pleated thread (*T*). $\times 9193$. Bar = $1.03 \mu\text{m}$

Fig. 15. Operculum (*O*) and flange (*F*) from holotranchous isorhiza. $\times 20000$. Bar = $0.25 \mu\text{m}$

Fig. 16. Discharged holotranchous isorhiza showing coiled tube (*T*) and spines (*S*). $\times 7500$. Bar = $1.2 \mu\text{m}$

Fig. 17. Longitudinal section through holotranchous isorhiza showing spines within undischarged tube and capsular matrix (*CM*). $\times 5560$. Bar = $0.9 \mu\text{m}$. *Inset*: Transverse section through holotranchous spine. $\times 60000$

Fig. 18. Partially discharged atrichous isorhiza capsule. $\times 3750$. Bar = $1.6 \mu\text{m}$

Fig. 19. Basal portions of discharged tubes (*T*) of 2 atrichous isorhizas, each surrounded by circular flange (*F*). $\times 11000$. Bar = $0.7 \mu\text{m}$

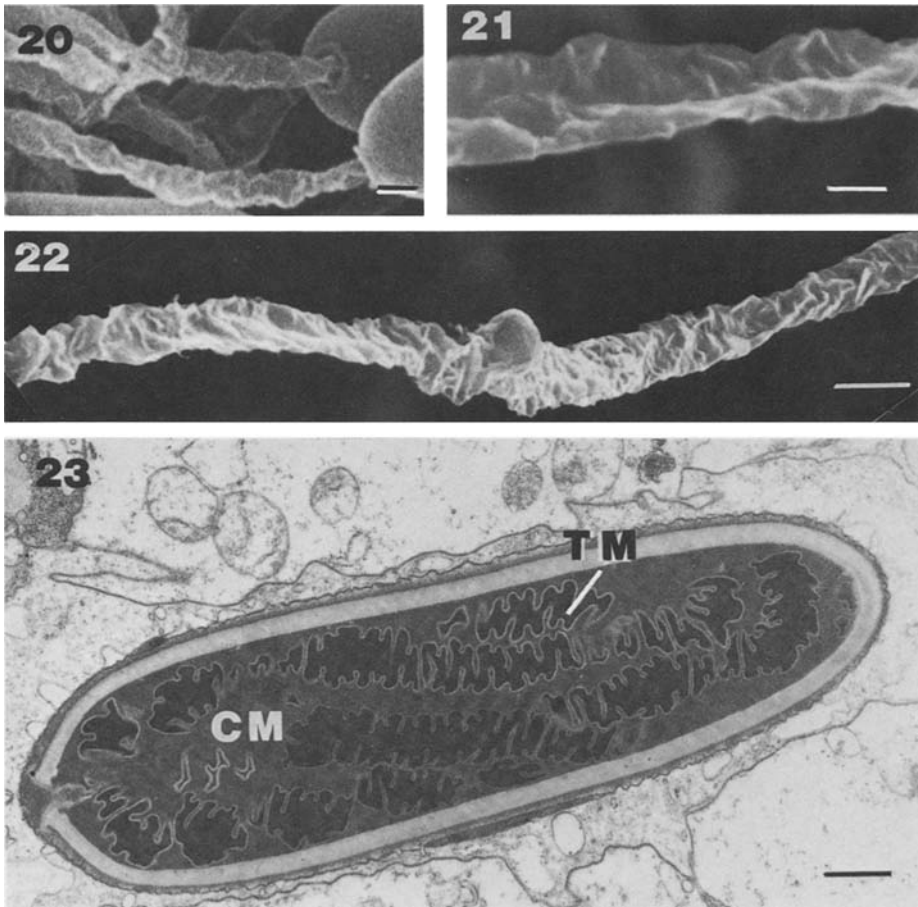


Fig. 20. Discharged tubes of 2 atrichous isorhizas from above (Fig. 19) capsules. $\times 3937$. Bar = $0.45 \mu\text{m}$

Fig. 21. Scanning electron micrograph from the middle portion of a discharged atrichous isorhiza tube. Spines and scars from broken spines are absent. $\times 8256$. Bar = $1.57 \mu\text{m}$

Fig. 22. Scanning electron micrograph from the mid-portion of a discharged atrichous isorhiza tube. Spines and scars from broken spines are absent on the buckled tube. $\times 5000$. Bar = $2 \mu\text{m}$

Fig. 23. Longitudinal section through an atrichous isorhiza. Note tube matrix (TM), capsular matrix (CM). Note absence of spines within inverted tube. $\times 7000$. Bar = $0.7 \mu\text{m}$

are more spherical than those of the larger euryteles. The flange surrounding the tripartite flap is not as protuberant as the flange of the large size category of euryteles. Upon discharge, three bulbous sections of the butt were apparent. The bulbous section nearest the operculum is the first to emerge. It is devoid of spines as is the third bulbous section. The second bulbous section possesses prominent spines which were curved in cross section

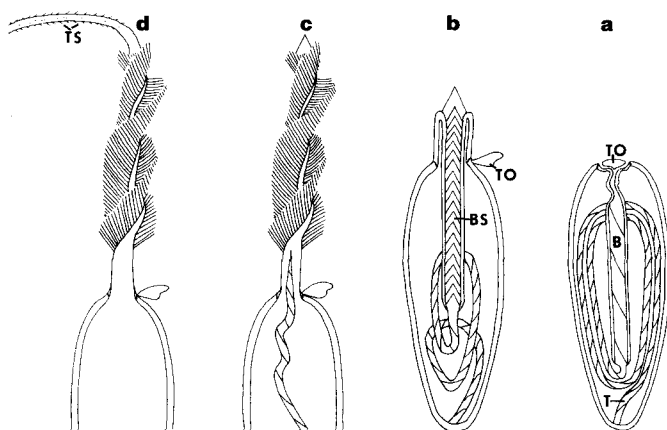


Fig. 24 a–d. Simplified schematic diagram of the stages of eversion of a microbasic mastigophore from *Chironex fleckeri*. **a** Undischarged capsule showing occluding tripartite operculum (*TO*), helically coiled, unpleated butt (*B*). Note thread (*T*) attached to the wall of the capsule at its narrow end. **b** Partially discharged microbasic mastigophore showing tripped operculum (*TO*) with butt spines (*BS*) attached to inside of butt wall, pointing towards apical end of capsule. Note butt spines just beginning to appear, forming a spear. **c** Partially discharged microbasic mastigophore with butt fully discharged. **d** Fully discharged microbasic mastigophore. Note 3 rows of thread spines (*TS*)

(Fig. 13). The spines are of similar size, up to 8 μm in length. After the butt appears the thread bearing fine barbs emerges. The length of the butt of euryteles of the larger category is usually about the same length as the capsule. The thread ranges from 590 to 790 μm in length and is usually about 20 times the capsule length. The butt of the euryteles of the small-sized category is also about the same length as the capsule but the thread ranges from 72 to 181.5 μm and is usually about 12 times the capsule length.

With Mallory's stain the capsular matrix in some small heterotrichous microbasic eurytele capsules was light blue, though some stained bright red. The capsule and tube stained light blue. The capsular matrix of large euryteles stained dark blue.

Holotrichous isorhizas

These nematocysts possess ellipsoidal capsules (Fig. 26a) having a mean long axis of 15 μm and a mean short axis of 8.0 μm (100 measurements). They are characterized by the presence of a spirally wound tube inside the capsule. The tube is devoid of a butt, is of uniform diameter (about 1.5 μm) and possesses spines throughout its length.

Electron microscopy revealed an operculum that is circular in outline (Fig. 15). The helically arranged spines are roughly triangular in shape. Fine tubules are present within the spines (Fig. 17 inset). When discharged the thread generally assumes the form of a spiral (Figs. 16, 26b), but is occasionally straight. The capsular matrix is generally of moderate electron

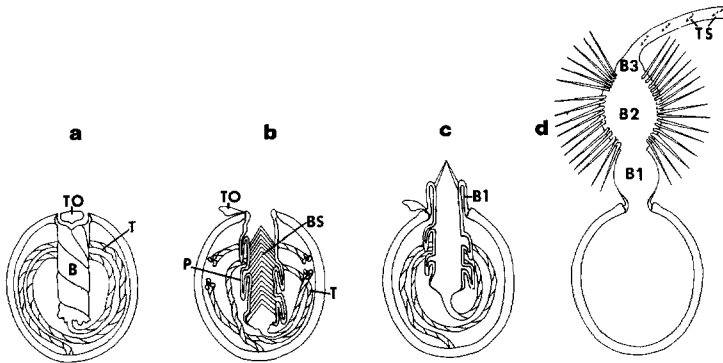


Fig. 25a–d. Simplified schematic diagram of stages in the eversion of a heterotrichous microbasic eurytele of *Chironex fleckeri*. **a** Undischarged eurytele of the small size category showing occluding tripartite operculum (*TO*), and deeply pleated butt (*B*). Note thread (*T*) attached to wall of the undischarged capsule. **b** Capsule of small size category of eurytele showing tripped tripartite operculum (*TO*). Note deep pleats (*P*) of butt, large spines (*BS*) pointing towards apical end of capsule, and triply pleated thread (*T*). **c** Partially discharged eurytele with first, spineless bulb (*B1*) having emerged. Note spear formation of emerging butt spines. **d** Fully discharged eurytele showing 3 bulbs of butt region, the first with no spines (*B1*), the second (*B2*) bearing long spines, the third devoid of spines (*B3*). Note spines on thread (*TS*)

density (Fig. 17). Under the TEM, the granular matrix within the tube is of medium to high electron density. There was comparatively little capsular matrix within the holotrichs examined.

With Mallory's stain the capsule and tube stained light blue whilst the capsular matrix was light mauve.

Atrichous isorhizas

Small cylindrical nematocysts (Fig. 18) possessing threads which are of uniform diameter throughout and without spines have been referred to the atrichous isorhiza category. The capsules (100 measurements) range from 5 to 17 μm in length (mean = 12.5 μm) and from 1.7 to 5 μm (mean = 3.7 μm) in diameter. The tube is approximately 1 μm in diameter and, when discharged, is usually 12–14 times the capsule length, ranging from 60 μm to 258 μm in length.

SEM reveals the presence of a small operculum, circular in outline, at one end of the atrichous isorhiza. The tubes of discharged atrichous isorhizas are usually buckled when discharged and lack spines as well as a butt (Figs. 19, 20, 21, 22, 27c).

Studies with TEM revealed that there is comparatively little pleating of the tube within the capsule but that folding occurs (Figs. 23, 27a, b). At times moderately electron-dense material is visible within the capsule and a large amount of strongly electron-dense material is packed within the tube (Fig. 23). At other times strongly electron-dense material is present

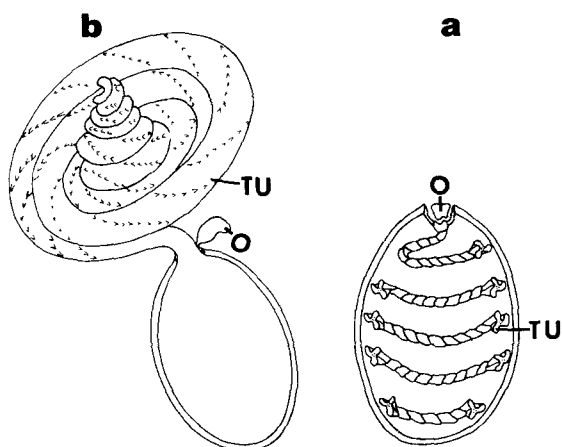


Fig. 26a, b. Simplified schematic diagram of **a** an undischarged ellipsoidal holotrichous isorhiza, showing occluding operculum (*O*) and triply pleated tube (*TU*). **b** A discharged holotrich showing the tripped operculum (*O*) and the coiled, spiny tube (*TU*)

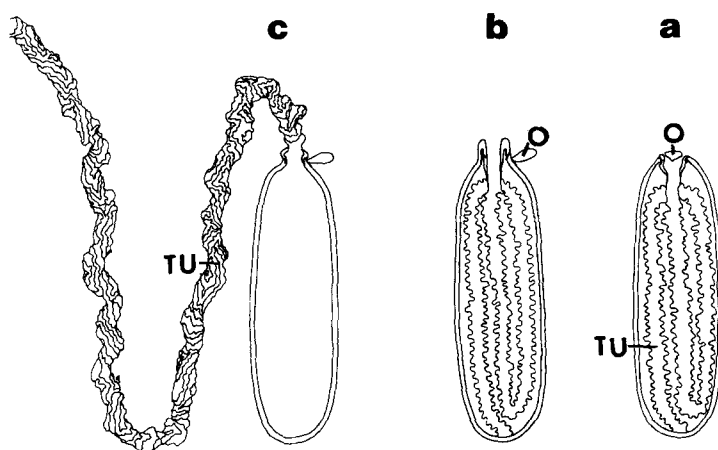


Fig. 27a-c. Simplified schematic diagram of stages of eversion of an atrichous isorhiza from *Chironex fleckeri* showing **a** occluding operculum (*O*) and folded, unpleated tube (*TU*). **b** Partially discharged atrich showing tripped operculum (*O*). **c** Fully discharged atrich showing buckling of atrich tube (*TU*)

within the capsule and moderately electron-dense material within the tube. Frequently the end of the tube is attached to the wall inside the capsule (Figs. 23, 27a, b).

With Mallory's stain the capsule and thread both stained light blue. The colour of the tube matrix, as seen through the capsule wall, varied between blue and red. Variations in staining properties were probably related to the maturity of the nematocysts.

Discussion

Kingston and Southcott (1960) found that the cubomedusan *Chironex fleckeri* possessed nematocysts of the microbasic mastigophore category. The cnidom of *C. fleckeri* was subsequently determined by Endean et al. (1969) who found it to be comprised of microbasic mastigophores (microbasic p-mastigophores of Carlgren 1940), microbasic euryteles, holotrichous isorhizas and atrichous isorhizas. The present study has confirmed the presence of these four basic types of nematocyst and has provided details of their ultrastructure.

Werner (1973, 1975) noted that the life histories of jellyfish of the family Cubomedusae differed markedly from those of jellyfish of other families, and suggested that the cubomedusans be placed in a new class of cnidarians, the class Cubozoa. Calder and Peters (1975) reported that the nematocyst complement of a cubomedusan, *Chiropsalmus quadrumanus*, contains microbasic mastigophores, heterotrichous microbasic euryteles and isorhizas. Further, they noted that microbasic mastigophores were present in other cubomedusans. Although microbasic mastigophores are commonly found among the nematocysts of anthozoans and hydrozoans they do not occur in scyphozoan jellyfish. Hence Calder and Peters suggested that the presence of mastigophores in the cnidom is a diagnostic feature of jellyfish of the class Cubozoa enabling them to be distinguished readily from jellyfish of the class Scyphozoa.

It was established that mature microbasic mastigophores of *C. fleckeri* possess spines on their tubes. They have penetrating and injecting functions. Those mastigophores possessing tubes devoid of spines noted by Endean et al. (1969) probably represent immature stages in the development of microbasic mastigophores. At times, developing nematocysts appear to predominate over fully developed nematocysts in material obtained from some tentacles. The origin and development of tentacular nematocysts is being investigated.

The present study has revealed the presence of a granular matrix inside the tube of the undischarged mastigophore. This matrix bathes the spines and is concentrated within the folds of the thread and in the butt region of the undischarged tube. It is possible that this matrix is not continuous with the matrix found within the capsule as, in some cases at least, the end of the thread distal to the butt did not appear to be open when the tube was in the inverted state.

Upon discharge the butt region everts first. The large spines of each nematocyst are arranged in 3 helices and point in the direction of discharge. Their arrangement differs from that of anthozoan microbasic mastigophores, as described by Westfall (1965), in that no pleats or pockets in which the spines are held in the undischarged state are visible in electron micrographs. The spines appear to act initially as a spike facilitating penetration of the butt. As the butt everts further the spines open outwards and probably serve to anchor the butt in the flesh of a victim. Next the tightly coiled and pleated thread everts. As it everts it rotates. This would enable

successive thread spines to participate in cutting a path through the flesh of a victim. When fully everted the tube is capable of penetrating to depths of about 500 μm .

If the granular matrix within the butt and thread of the tube is venom it is likely that this material is injected continuously as the tube inverts and penetrates flesh, a possibility that has already been raised by Cormier and Hessinger (1980) for holotrichous isorhizas of *Physalia physalis* and by Tardent and Holstein (1982) for stenoteles of *Hydra attenuata*. This mode of envenomation does not preclude the release of intracapsular material through the hollow tube at some stage during eversion of the tube. However, some or all of the material within the tube would normally be released before the intracapsular material. It remains to be seen whether material inside the inverted tube, which comes to lie on the outside of the everted tube, is different from the material in the undischarged capsule, particularly with respect to toxicity.

Microbasic euryteles of two size groups were found among the nematocysts of *C. fleckeri* by Endean et al. (1969). The present study has confirmed the presence of these two distinct size groups and has revealed differences in the appearance of representatives of the two groups enabling them to be regarded as two distinct varieties. However, both varieties of eurytele can be placed in the category of heterotrichous microbasic euryteles of Weill (1934). Scyphozoans possess euryteles similar to those of the smaller size range found in *C. fleckeri*, but large euryteles similar to those belonging to the larger size range found in *C. fleckeri* appear to be lacking in scyphozoans. Such large euryteles are present in *Chiropsalmus quadrumanus*, *Carybdea rastoni* and *Carukia barnesi* (Southcott 1967) and their presence may represent another diagnostic feature of the class Cubozoa.

Judging by their structure, the euryteles of *C. fleckeri* would appear to be both penetrants and injectors. No information suggesting a specific role for euryteles was obtained. The work of Endean and Rifkin (1975) on isolated nematocyst types indicates that different toxins are elaborated in mastigophores and euryteles respectively in *C. fleckeri* and that the euryteles do not appear to play a major role in mammalian envenomations although they are undoubtedly capable of penetrating the skin. The great length of the thread and the relatively large size of the butt spines suggest that the large euryteles might be effective in binding prey to the tentacles.

The presence of tripartite opercula in heterotrichous microbasic euryteles and in microbasic mastigophores of *C. fleckeri* is a departure from the typical structure of scyphozoan nematocysts. In scyphozoan nematocysts a circular operculum is present (Mariscal 1974). The existence of tripartite flaps in some types of nematocyst of *C. fleckeri* can be added to the list of features distinguishing the class Cubozoa from the class Scyphozoa.

Holotrichous isorhizas similar to those found in *C. fleckeri* have not been reported from other cubozoans. However, they may have been overlooked because they are relatively uncommon compared with the occurrence of other nematocyst types. Indeed, the "ovoid isorhizas" of *Chiropsalmus quadrumanus* mentioned by Calder and Peters (1975) may belong to this

category. Although they possess spines on a folded thread there is no evidence that the tubes of these nematocysts normally penetrate the skin of a victim. They may have primarily an entangling function as suggested by Endean et al. (1969) or have both an entangling and adhesive function. Certainly most adopt a spiral configuration when they discharge and the curved spines on the tubes would seem admirably suited to catching on the hairs and bristles of crustacean prey.

Nematocysts were placed by Weill (1934) in one of two basic categories – stomocnides and astomocnides. Among the various types of nematocyst described by Weill (1934) were the atrichous isorhizas of the stomocnide category. Nematocysts of the atrichous isorhiza type each possesses a tube that is devoid of spines and is of the same diameter throughout its length. Its tip is open. However, astomocnides which have closed tips may also possess tubes devoid of spines. Weill's observations of nematocyst structure were based on examination with the optical microscope. Subsequent use of the electron microscope by later workers failed to detect atrichous isorhizas. Indeed, according to Mariscal et al. (1977, p 402) "all atrichs examined to date with the electron microscope have been found to possess spines along their length and thus are actually holotrichous." However, no spines were detected in electron micrographs of a type of nematocyst occurring commonly in *C. fleckeri*. In nematocysts belonging to this type the tube appears to be open at the tip in some cases, at least. Hence these nematocysts have been placed in Weill's atrichous isorhiza type. However, it is not known whether the tip is open in all cases. Also, it is not known whether atrichous isorhizas occur in other cubomedusans.

The absence of spines militates against any penetrating function, and atrichous isorhizas have not been found among the nematocysts actually penetrating the skins of human victims of stinging by *C. fleckeri* material appears as the tube everts. It appears to be used to bring about an attachment of tentacle to prey and may have adhesive properties. Endean et al. (1969) have already suggested that the atrichous isorhizas have a glutinant action causing tentacles to adhere to prey or victims.

The information obtained in this study has implications for human envenomations and their treatment as well as for the preparation of toxin extracts for study. It would appear that of the different types of nematocyst present only mastigophores are of importance in human envenomations, as suggested earlier by Endean and Rifkin (1975). The possibility that the mastigophores inject venom continuously as they discharge rather than injecting venom only after the thread is fully everted requires reappraisals of the manner in which venom is introduced into the systemic circulation of mammals and of methods aimed at preventing the discharge of nematocysts in tentacles adhering to victims.

References

- Barnes JH (1966) Studies on three venomous Cubomedusae. Extraction of cnidarian venom from living tentacles. Symp Zool Soc London 16:307-332
- Calder DR, Peters EC (1975) Nematocysts of *Chiropsalmus quadrumanus* with comments on the systematic status of the Cubomedusae. Helgol Wiss Meeresunters 27:364-369

- Carlgren O (1940) A contribution to the knowledge of structure and distribution of cnidae in the Anthozoa especially in the Actinaria. Lunds Univ Arsskr Avd 2 (N.S.) 36:1–62
- Cleland JB, Southcott RV (1965) Injuries to man from marine invertebrates in the Australian region. Commonwealth of Australia, Canberra A.C.T. pp 43–116
- Cormier SM, Hessinger DA (1980) Cellular basis for tentacle adherence in the Portuguese man-of-war (*Physalia physalis*). Tissue Cell 12:713–721
- Endean R (1981) The box jelly-fish or “sea-wasp”. In: Pearn J (ed) Animal toxins and man. Human poisoning by toxic Australian venomous creatures. Queensland Health Department, Brisbane, pp 46–54
- Endean R, Duchemin C, McColm D, Fraser EH (1969) A study of the biological activity of toxic material derived from nematocysts of the cubomedusan *Chironex fleckeri*. Toxicon 6:179–204
- Endean R, Rifkin J (1975) Isolation of different types of nematocyst from the cubomedusan *Chironex fleckeri*. Toxicon 13:375–376
- Kingston CW, Southcott RV (1960) Skin histopathology in fatal jellyfish stinging. Trans R Soc Trop Med Hyg 54:373–383
- Mariscal RN (1974) Nematocysts. In: Muscatine L, Lenhoff HM (eds) Coelenterate biology: reviews and new perspectives. Academic Press, New York, pp 129–178
- Mariscal RN, Conklin EJ, Bigger CH (1977) The ptychocyst, a new major category of cnida used in tube construction by a cerianthid anemone. Biol Bull (Woods Hole) 152:392–405
- Picken LER, Skaer RJ (1966) A review of researches on nematocysts. Symp Zool Soc London 16:19–50
- Southcott RV (1967) Revision of some Carybdeidae (Scyphozoa: Cubomedusae), including a description of the jelly fish responsible for the “Irukandji Syndrome”. Aust J Zool 15:651–671
- Spurr AR (1969) A low-viscosity epoxy resin embedding medium for electron microscopy. J Ultrastruct Res 26:31–43
- Tardent P, Holstein T (1982) Morphology and morphodynamics of the stenotele nematocyst of *Hydra attenuata* Pall (Hydrozoa, Cnidaria). Cell Tissue Res 224:269–290
- Weill R (1934) Contribution à l'étude des cnidaires et le leurs nematocystes. I. Trav Sta Zool Wimereux 10:1–347
- Werner B (1973) New investigations on the systematics and evolution of the class Scyphozoa and the phylum Cnidaria. Publ Seto Mar Biol Lab 20:35–61
- Werner B (1975) Bau- und Lebensgeschichte von *Tripedalia cystophora* (Cubozoa). Helgoländer wiss Meeresunters 27:461–504
- Westfall JA (1965) Nematocysts of the sea anemone *Metridium*. Amer Zoologist 6:377–393
- Williamson JA, Callanan VI, Hartwick RF (1980) Serious envenomation by the northern Australian box-jellyfish (*Chironex fleckeri*). Med J Aust 1:13–15